



ELSEVIER

Journal of Alloys and Compounds 330–332 (2002) 458–461

Journal of  
ALLOYS  
AND COMPOUNDS

www.elsevier.com/locate/jallcom

# Comparison of the dynamics of hydrogen and deuterium dissolved in crystalline $\text{Pd}_9\text{Si}_2$ and $\text{Pd}_3\text{P}_{0.8}$

T.J. Udovic<sup>a,\*</sup>, C. Karmonik<sup>a</sup>, Q. Huang<sup>a,b</sup>, J.J. Rush<sup>a</sup>, M. Vennström<sup>c</sup>, Y. Andersson<sup>c</sup>,  
T.B. Flanagan<sup>d</sup>

<sup>a</sup>NIST Center for Neutron Research, National Institute of Standards and Technology, 100 Bureau Dr., MS 8562, Gaithersburg, MD 20899-8562, USA

<sup>b</sup>Department of Materials and Nuclear Engineering, University of Maryland, College Park, MD 20742, USA

<sup>c</sup>Department of Inorganic Chemistry, University of Uppsala, S-751 21, Uppsala, Sweden

<sup>d</sup>Department of Chemistry, University of Vermont, Burlington, VT 05405, USA

## Abstract

The bonding potentials of hydrogen and deuterium dissolved in the crystalline alloys  $\text{Pd}_9\text{Si}_2$  and  $\text{Pd}_3\text{P}_{0.8}$  have been studied by neutron scattering techniques. Neutron powder diffraction verifies that, in both alloys, the principal type of interstitial absorption site is the quadrilateral base of a Pd-defined pyramid situated on the face of an empty triangular prism. The neutron vibrational spectroscopy results indicate that, although the H and D vibrational energies parallel to the Pd pyramidal base appear to be similar for both alloys, the H and D vibrational energies perpendicular to the Pd pyramidal base for  $\text{Pd}_9\text{Si}_2$  are  $\approx 15\%$  softer than the corresponding energies for  $\text{Pd}_3\text{P}_{0.8}$ . Both neutron vibrational spectroscopy and quasielastic neutron scattering show that hydrogen hopping between the two pyramidal absorption sites associated with different faces of the same prism is much more rapid in  $\text{Pd}_9\text{Si}_2$  than in  $\text{Pd}_3\text{P}_{0.8}$ . This may be directly attributable to the observed softer potential along the hopping trajectory (i.e. perpendicular to the Pd pyramidal base) for the interstitial site in  $\text{Pd}_9\text{Si}_2$  compared to that in  $\text{Pd}_3\text{P}_{0.8}$ . © 2002 Elsevier Science B.V. All rights reserved.

**Keywords:** Hydrogen; Palladium; Silicon; Phosphorus; Vibrations; Neutron scattering

## 1. Introduction

Although palladium–hydrogen has been among the most studied of all metal–hydrogen systems, much less emphasis has been placed on characterizing the hydrogen interactions with Pd compounded with non-metallic elements. Nonetheless, knowledge of the physicochemical behavior of these Pd compounds is of potential interest in such areas as the semiconductor industry, where Pd is a technologically important material and non-metallic contaminants are always of concern.

In the past, studies of the palladium–silicon [1–5] and palladium–phosphorus [6–14] systems have been undertaken to explore the interesting structural and thermodynamic properties of these alloys. Two different crystalline orthorhombic (*Pnma*) alloys,  $\text{Pd}_9\text{Si}_2$  and  $\text{Pd}_3\text{P}_{1-u}$  ( $0 \leq u \leq 0.28$ ), are found to be of particular fundamental interest because they both dissolve hydrogen in solid

solution with the H atoms located primarily in geometrically similar, yet unusual interstitial sites.  $\text{Pd}_9\text{Si}_2$  is characterized by an augmented triangular prismatic ten-fold coordination for Si, which occurs in several metal-rich transition-metal silicides, e.g. the  $\text{Co}_2\text{Si}$ -type structure [1].  $\text{Pd}_3\text{P}_{1-u}$  crystallizes with the cementite  $\text{Fe}_3\text{C}$ -type structure, possessing distorted triangular prismatic  $\text{Pd}_6$  building blocks similar to  $\text{Pd}_9\text{Si}_2$ , but with P atoms at the prism centers [7,14]. In both hydrogenated alloys, the H atoms are known to reside mainly in one type of interstice, i.e. in the base of a  $\text{Pd}_5$  distorted square pyramidal site situated on the quadrilateral face of an empty triangular prism [4,7] (Fig. 1). For  $\text{Pd}_3\text{P}_{1-u}$ , this can only occur for  $u > 0$ , where  $u$  random vacancies exist at the otherwise occupied P positions. In this paper, a comparison of the bonding potentials of hydrogen and deuterium dissolved in the crystalline alloys  $\text{Pd}_9\text{Si}_2$  and  $\text{Pd}_3\text{P}_{0.8}$  (i.e.  $u = 0.2$ ) has been undertaken utilizing neutron scattering techniques. In particular, neutron powder diffraction (NPD), neutron vibrational spectroscopy (NVS), and quasielastic neutron scattering (QENS) have been used to characterize the

\*Corresponding author.

E-mail address: udovic@nist.gov (T.J. Udovic).

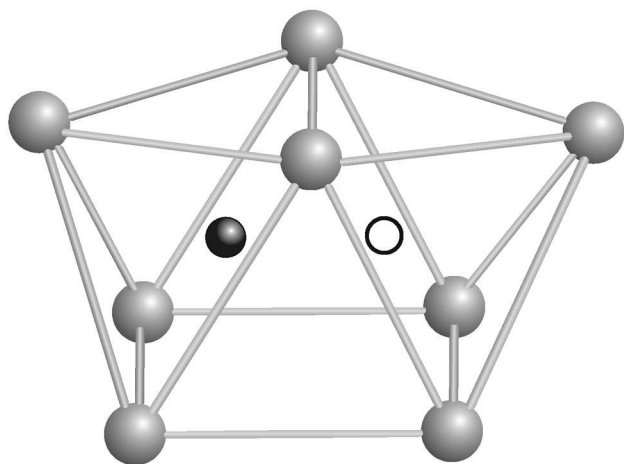


Fig. 1. The local Pd atom environment of an H atom in  $\text{Pd}_9\text{Si}_2$  and  $\text{Pd}_3\text{P}_{0.8}$ . The H atom (black sphere) has five near-neighbor Pd atoms (gray spheres) in a distorted square pyramidal site. The bases of such  $\text{Pd}_5$  pyramidal sites share two of the three quadrilateral faces of an empty  $\text{Pd}_6$  triangular prism. Only one of the two neighboring pyramidal sites is occupied at any one time. This provides the geometry for a hydrogen-hopping mechanism between the two sites.

location and dynamics of the hydrogen isotopes within the  $\text{Pd}_9\text{Si}_2$  and  $\text{Pd}_3\text{P}_{0.8}$  alloy matrices.

## 2. Experimental

Crystalline  $\text{Pd}_9\text{Si}_2$  ( $\approx 36$  g) and  $\text{Pd}_3\text{P}_{0.8}$  ( $\approx 33$  g) were synthesized as discussed elsewhere [1,7]. Finely powdered samples of each compound were sealed in Al tubular cells equipped with valves. Typically, hydrogen and deuterium were dissociatively absorbed by the samples from the gas phase at room temperature after evacuating any residual H or D at 373 K. All H and D uptakes were in agreement with previously measured solubility data [2,8].

All neutron scattering measurements were taken at the NIST Center for Neutron Research. NPD, NVS, and QENS data were collected on the BT-1 high-resolution powder diffractometer, the BT-4 filter-analyzer spectrometer, and the Fermi-chopper time-of-flight spectrometer, respectively. The instrumental resolutions (full widths at half maximum, FWHM) of the NVS data in the figures are denoted by horizontal bars beneath the spectra.

## 3. Results and discussion

NPD patterns collected for  $\text{Pd}_9\text{Si}_2\text{D}_{0.25}$  and  $\text{Pd}_3\text{P}_{0.8}\text{D}_{0.15}$  at 10 and 296 K verified the previously reported crystalline structures and confirmed that the D atoms primarily occupied the base of  $\text{Pd}_5$  pyramidal sites. Fig. 2 illustrates a comparison of the low-temperature ( $\leq 20$  K) H and D density-of-states (DOS) spectra for  $\text{Pd}_9\text{Si}_2\text{H}_{0.25}$ ,  $\text{Pd}_3\text{P}_{0.8}\text{H}_{0.16}$ ,  $\text{Pd}_9\text{Si}_2\text{D}_{0.25}$ , and  $\text{Pd}_3\text{P}_{0.8}\text{D}_{0.15}$  obtained by

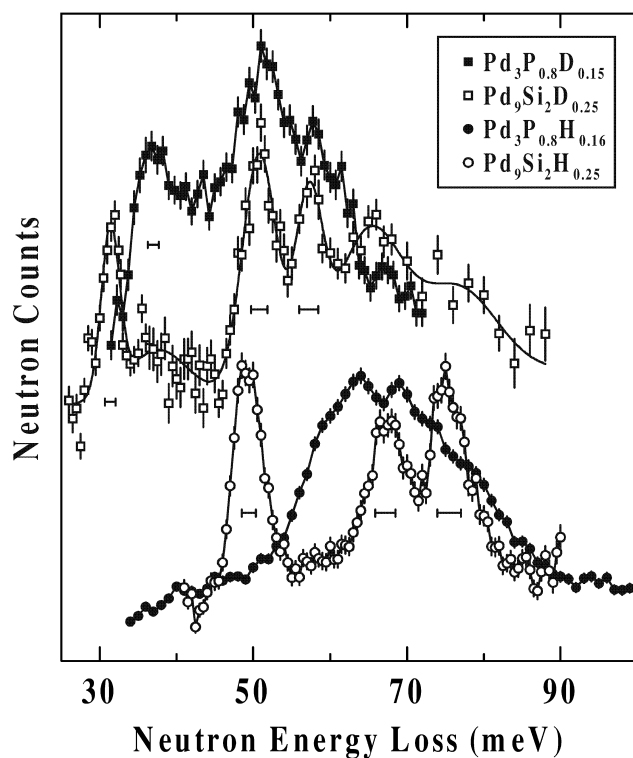


Fig. 2. Comparison of the low-temperature ( $\leq 20$  K) H and D DOS spectra for hydrogenated and deuterated  $\text{Pd}_9\text{Si}_2$  and  $\text{Pd}_3\text{P}_{0.8}$ .

NVS. A previous discussion [3] of the  $\text{Pd}_9\text{Si}_2\text{H}_{0.25}$  and  $\text{Pd}_9\text{Si}_2\text{D}_{0.25}$  spectra has assigned the three well-defined optic vibrational features located at 49.4, 67.2, and 75.5 meV (for  $\text{Pd}_9\text{Si}_2\text{H}_{0.25}$ ) and at 31.4, 50.8, and 57.2 meV (for  $\text{Pd}_9\text{Si}_2\text{D}_{0.25}$ ) to the three normal-mode vibrations associated with the pyramidal site. In each case, the softest mode is attributed to the vibration perpendicular to the pyramidal base, and the two higher-energy modes are attributed to the two orthogonal normal-mode vibrations parallel to this base. The non-degeneracy found for these higher-energy modes reflects the non-square distortion of the pyramidal base. (For  $\text{Pd}_9\text{Si}_2\text{D}_{0.25}$ , additional scattering intensity found at higher energies above 60 meV is attributed to overtones, multiphonon scattering, and the possibility of residual H in the deuterated sample.) A comparison of the H and D normal-mode energies gives H/D energy ratios of 1.57 for the low-energy and 1.32 for both higher-energy modes, reflecting an unusual potential for the  $\text{Pd}_9\text{Si}_2$  pyramidal site, especially along the trajectory perpendicular to the pyramidal base.

Although the pyramidal absorption site geometries are similar for  $\text{Pd}_9\text{Si}_2$  and  $\text{Pd}_3\text{P}_{0.8}$ , the H and D vibrational spectra for  $\text{Pd}_3\text{P}_{0.8}\text{H}_{0.16}$  and  $\text{Pd}_3\text{P}_{0.8}\text{D}_{0.15}$  in Fig. 2 clearly display differences with the  $\text{Pd}_9\text{Si}_2\text{H}_{0.25}$  and  $\text{Pd}_9\text{Si}_2\text{D}_{0.25}$  spectra. First, the H and D vibrational features for  $\text{Pd}_3\text{P}_{0.8}\text{H}_{0.16}$  and  $\text{Pd}_3\text{P}_{0.8}\text{D}_{0.15}$  are relatively broader compared to those for  $\text{Pd}_9\text{Si}_2\text{H}_{0.25}$  and  $\text{Pd}_9\text{Si}_2\text{D}_{0.25}$ , which is most likely reflective of the innate differences in the two

crystallographic structures. In particular, all Pd and Si atoms in the  $\text{Pd}_9\text{Si}_2$  structure are situated at well-defined crystallographic positions with full occupancies. This means that all primary pyramidal absorption sites have a unique extended environment of neighboring Pd and Si atoms. In contrast, the vacancy (and P) disorder resulting from the P-deficient  $\text{Pd}_3\text{P}_{0.8}$  structure leads to pyramidal absorption sites with a unique extended environment of neighboring Pd atoms, yet also with a distribution of different neighboring P-atom arrangements. This results in a distribution of absorption-site potentials and has the effect of broadening the normal-mode peaks.

Assuming that the spectra for the P-based system similarly reflect the three normal modes of the pyramidal absorption site, it is immediately evident that the two higher-energy features at  $\approx 51$  and  $57.8$  meV are very similar to the analogous mode energies for  $\text{Pd}_9\text{Si}_2\text{D}_{0.25}$  and can likewise be attributed to the two non-degenerate orthogonal normal-mode vibrations parallel to the pyramidal base. In contrast, the lowest-energy feature at  $\approx 37$  meV for  $\text{Pd}_3\text{P}_{0.8}\text{D}_{0.15}$ , which can be attributed to the normal-mode vibration perpendicular to the pyramidal base, is nearly 6 meV higher in energy than the analogous feature for  $\text{Pd}_9\text{Si}_2\text{D}_{0.25}$ .

The normal-mode peaks of the  $\text{Pd}_3\text{P}_{0.8}\text{H}_{0.16}$  vibrational spectra are largely overlapping and yield a single broad vibrational band. As such, it is more difficult to determine the exact energies of the normal-mode features, although the fine structure associated with this band suggests local peak maxima near 64 and 69 meV as well as spectral shoulders near 59, 74, and 78 meV. Taking the assigned D normal-mode energies for  $\text{Pd}_3\text{P}_{0.8}\text{D}_{0.15}$  and calculating the H normal-mode energies for  $\text{Pd}_3\text{P}_{0.8}\text{H}_{0.16}$  with the assumed H/D energy ratios determined from the  $\text{Pd}_9\text{Si}_2$  system, yields values of 58, 67, and 76 meV. These values are in reasonable agreement with the general location and structure of the observed vibrational band, which is again indicative of a similarly unusual potential for the  $\text{Pd}_3\text{P}_{0.8}$  pyramidal site. It is probable that the murky nature of the observed H vibrational band is another consequence of the details associated with the disordered P-atom distribution within the  $\text{Pd}_3\text{P}_{0.8}$  structure. Such details must be taken into account for a more quantitative analysis of the observed distribution of normal-mode energies.

Fig. 3 illustrates the difference in the temperature dependence of the vibrational spectra for  $\text{Pd}_9\text{Si}_2\text{H}_{0.25}$  and  $\text{Pd}_3\text{P}_{0.8}\text{H}_{0.16}$ . In particular, for  $\text{Pd}_9\text{Si}_2\text{H}_{0.25}$ , a substantial spectral smearing occurs at room temperature, significantly raising the entire baseline scattering, and suggesting the onset of diffusive hydrogen motion. For  $\text{Pd}_3\text{P}_{0.8}\text{H}_{0.16}$ , the spectral smearing is less substantial and characteristic of a normal temperature-induced attenuation due to an increased Debye-Waller factor. Moreover for both systems, a shifting at high temperatures of some of the main band intensities to lower energies is expected. The behavior of the  $\text{Pd}_9\text{Si}_2\text{H}_{0.25}$  spectrum is consistent with previously

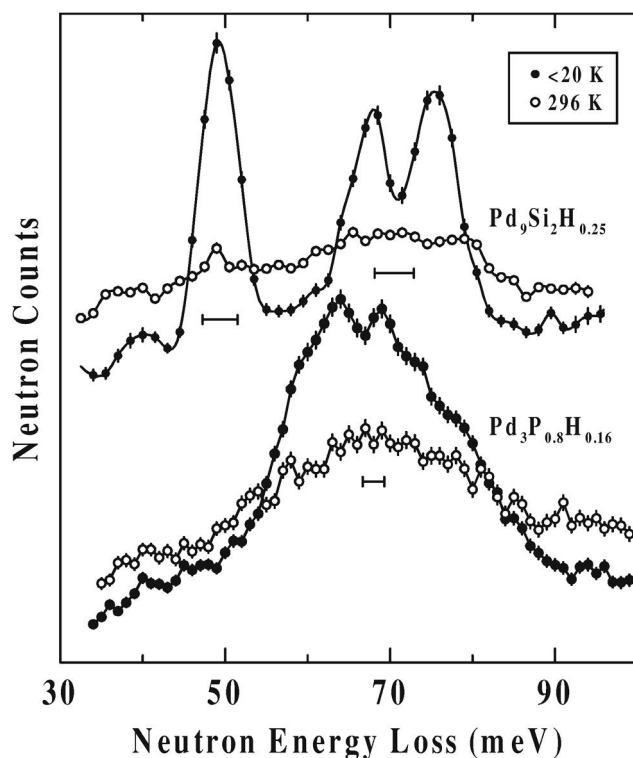


Fig. 3. Comparison of the temperature dependence of the H DOS spectra for hydrogenated  $\text{Pd}_9\text{Si}_2$  and  $\text{Pd}_3\text{P}_{0.8}$ .

reported QENS measurements indicating the presence of significant H hopping motion (on the order of  $10^{11}$  jumps/s) at room temperature between adjacent pyramidal sites [4,5]. The corresponding double-well potential was found to be asymmetric, which is in accordance with the crystallographic inequivalence of the two sites. The more stable site is 0.317 nm away from the nearest Si atom, whereas the less stable site is only 0.288 nm away from the nearest Si atom. The behavior of the  $\text{Pd}_3\text{P}_{0.8}\text{H}_{0.16}$  spectrum is also consistent with QENS measurements, which show no measurable quasielastic line broadening at room temperature with an elastic peak resolution of  $68 \mu\text{eV}$  FWHM. Although previous neutron scattering measurements [11] of the hydrogen Debye-Waller factor for  $\text{Pd}_3\text{P}_{0.8}\text{H}_{0.2}$  at 400 and 515 K suggested the presence of H oscillatory motions between the two pyramidal sites, it is clear from the present NVS and QENS measurements that the room temperature frequency of such motions is orders-of-magnitude smaller for H in  $\text{Pd}_3\text{P}_{0.8}$  than for H in  $\text{Pd}_9\text{Si}_2$ .

From these results, it appears that there are significant alloy-dependent differences in the potential along the hopping trajectory within the  $\text{Pd}_6$  prisms in these compounds. The direction of this trajectory is similar to the direction of the large-amplitude hydrogen normal-mode vibration perpendicular to the pyramidal base. It is interesting to note that the alloy with the higher H hopping frequencies ( $\text{Pd}_9\text{Si}_2\text{H}_x$ ) also displays a lower energy for this normal mode. It can be argued that this is to be

expected since a lower vibrational energy means a softer potential well. To first order, the softness of the two potential wells (associated with the two pyramidal sites) that combine to form the potential energy surface for hopping will directly effect the magnitude of the activation-energy barrier between the wells. The combination of softer wells will likely result in lower hopping barriers, which is consistent with the more rapid hopping observed for  $\text{Pd}_9\text{Si}_2\text{H}_x$ .

#### 4. Conclusions

The bonding potentials of hydrogen and deuterium dissolved in the crystalline alloys  $\text{Pd}_9\text{Si}_2$  and  $\text{Pd}_3\text{P}_{0.8}$  have been studied by neutron scattering techniques. Neutron powder diffraction, neutron vibrational spectroscopy, and quasielastic neutron scattering have been used to characterize the location and dynamics of the hydrogen isotopes within the alloy matrices. In both alloys, hydrogen is located primarily within the base of an unusual pyramidal site comprised of five Pd atoms, yet neutron scattering results indicate significant alloy-dependent differences in the hydrogen bonding potentials and hopping dynamics. In particular, although the H and D vibrational energies parallel to the Pd pyramidal base appear to be similar for both alloys, the H and D vibrations perpendicular to the Pd pyramidal base for  $\text{Pd}_9\text{Si}_2$  are  $\approx 15\%$  softer than the corresponding modes for  $\text{Pd}_3\text{P}_{0.8}$ . This softer potential for  $\text{Pd}_9\text{Si}_2$  probably reflects the relatively greater ease for two-site hydrogen hopping along this trajectory in  $\text{Pd}_9\text{Si}_2$

compared to that in  $\text{Pd}_3\text{P}_{0.8}$ . Ab initio calculations are planned to elucidate the primary perturbations of neighboring Si and P atoms that lead to such alloy-dependent potential differences between otherwise geometrically similar interstitial hydrogen sites.

#### References

- [1] Y. Andersson, Chem. Scripta 28 (1988) 125.
- [2] T.B. Flanagan, H. Noh, A. Craft, Y. Andersson, J. Solid State Chem. 120 (1995) 90.
- [3] T.J. Udovic, J.J. Rush, T.B. Flanagan, H. Noh, Y. Andersson, J. Alloys Comp. 253–254 (1997) 255.
- [4] C. Karmonik, T.J. Udovic, Q. Huang, J.J. Rush, Y. Andersson, T.B. Flanagan, Physica B 241–243 (1998) 332.
- [5] C. Karmonik, Q. Huang, T.J. Udovic, J.J. Rush, Y. Andersson, T.B. Flanagan, Mat. Res. Soc. Symp. Proc. 527 (1988) 75.
- [6] Y. Andersson, Acta Chem. Scand. A31 (1977) 354.
- [7] Y. Andersson, S. Rundqvist, R. Tellgren, J.O. Thomas, T.B. Flanagan, J. Solid State Chem. 32 (1980) 321.
- [8] T.B. Flanagan, G.E. Biehl, J.D. Clewley, S. Rundqvist, Y. Andersson, J. Chem. Soc. Faraday Trans. 1 76 (1980) 196.
- [9] Y. Andersson, S. Rundqvist, R. Tellgren, J.O. Thomas, T.B. Flanagan, Acta Crystallogr. B37 (1981) 1965.
- [10] T.B. Flanagan, B.S. Bowerman, S. Rundqvist, Y. Andersson, J. Chem. Soc. Faraday Trans. 1 79 (1983) 1605.
- [11] D. Noreus, U. Dahlborg, Y. Andersson, R. Tellgren, Solid State Commun. 46 (1983) 553.
- [12] Y. Andersson, S. Rundqvist, R. Tellgren, J. Solid State Chem. 52 (1984) 327.
- [13] Y. Andersson, S. Rundqvist, R. Tellgren, T.B. Flanagan, Z. Phys. Chem. N. F. 145 (1985) 43.
- [14] Y. Andersson, Chem. Scripta 26A (1986) 99.